Millimeter wave standoff radar detection system with motion compensation and 3D imaging capabilities

Galia Ghazi, Fernando Quivira, Jose A. Martinez and Carey M. Rappaport

Department of Electrical and Computer Engineering, Northeastern University, Boston, MA 02115 (ghazi.g@husky.neu.edu)

Introduction

The mm-waves radar is the ideal modality for standoff detection because it can work at distances from 20 to 50 meters. In addition mm-waves can penetrate clothing, and have high resolving capability reacting to the dielectric contrast of interest (explosives). In this poster we present our latest results in the area of standoff detection of potential suicide bombers using millimeter wave radar. We have collected experimental data using a mm-wave radar, with a multiple bistatic configuration. The data has been processed, by using a Synthetic Aperture Radar (SAR) technique, in order to create two dimensional images on the target region. Then, a feature algorithm based on entropy level has been applied to the SAR image in order to distinguish between threat and no threat cases. This SAR has a moving rail over a linear aperture of 1.85m and has Frequency Modulated Continuous Wave (FMCW) signal. In this work we have implemented a new motion compensation algorithm in order to improve the SAR images generated from the measured data with different threat objects. The algorithm corrects for the relative movement existing between the target and the radar system by using a corner cube reference in the target region. This method improves the imaging accuracy and the capability for distinguishing threat from innocent cases. This poster also presents simulated results for a possible extended version of mm-wave standoff radar configuration which would have the potential for 3D imaging capabilities. For this purpose, the system consists of a two-dimensional aperture array of receivers, which ultimately improves the detection performance of potential hazards.

Radar Configuration

We use the SAR image processing of the measurements from a FMCW radar. The Radar has the following parameters: center frequency=94.2GHz, bandwidth=4GHz and pulse burst duration= 83.36μs.

- The radar system has both monostatic and bistatic receiving antennas Fig.1(a). The configuration of the measurement consists of a person, who is the target and a corner cube in the target region Fig.1(b).

Motion compensation algorithm

- The unknown relative movement of the target produces distortions in the final images. For compensating for these errors, three steps are used in the correction algorithm:
  1- Correction of the slight phase fluctuation occurring during the measurement in successive pulses.
  2- Optimize the measurement parameters using the bistatic data. Parameters are the corner cube position and the monostatic receiver position in Fig. 1(b).
  3- Compensate for the random phase error in the bistatic measured data with the phase of the monostatic measured data.
- With the knowledge of the position of the bistatic receiver $x(t)$, the optimization is performed. It is a nonlinear optimization algorithm, which uses the equation for the measured distance from the corner cube. This distance is shown in equation (1). The optimized parameters in this equation are the position of the transmitting antenna (x_1) and the position of the corner cube (x_0, y_0).

$$distance = \sqrt{(x_0 - x_1)^2 + y_0^2} + \sqrt{(x_0 - x(t))^2 + y_0^2} \qquad (1)$$

Results

By using the new optimized parameters and SAR image processing technique the measured data is processed to obtain the images. Photographs of test cases are shown in Fig.2. For distinguishing between threat and innocent targets the entropy criterion is utilized. Entropy is a statistical measure of randomness in the images and is as defined in equation (2). The parameter 'p' in this equation

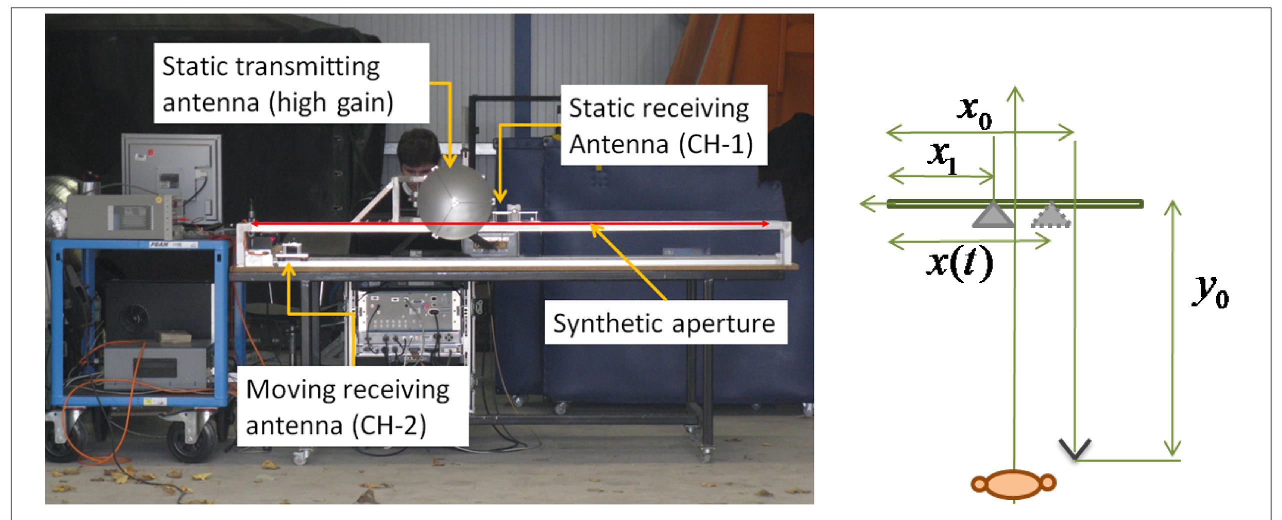

(a) (b)

Figure 1: (a) picture of the real radar (b) measurement configuration.

(a) (b) (c)

Figure 2: image of the target with different threats (a) with a silicon metallic object on the chest (b) with metallic pipes on the chest. (c) with a silicon pipes on the chest

contains the histogram counts of the 2-dimentional images that are the result of SAR processing.

$$entropy = -\sum p \cdot log(p) \qquad (2)$$

- In threat cases, the entropy is on average higher because of distribution of the hot spots in the images. As a result with introducing a threshold on the entropy of the images the threat detection is possible. The images for a male target without and with different type of threats on his chest are shown in Fig.3. The entropy calculated for each of the images is depicted at its title.
- In Fig.3, the first image (a) is no threat, and images (b), (c), and (d) correspond to the objects depicted in Fig.2 (a), (b), and (c).

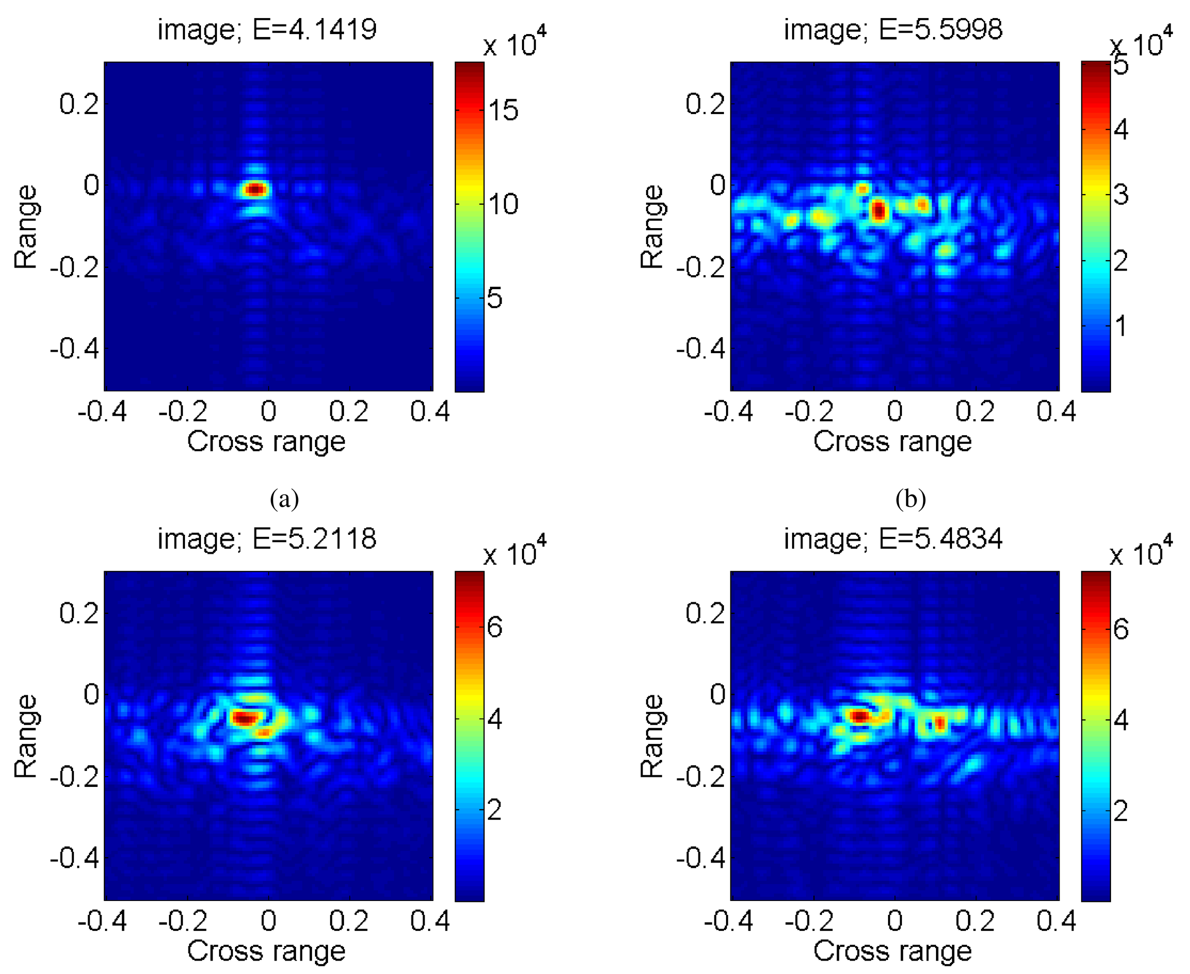

Figure 3: image of the target (a) without threat (b) with a silicon metallic object on the chest (c) with metallic pipes on the chest. (d) with a silicon pipes on the chest

- The entropy for the innocent case is 4.14, while for the threat cases it is (5.59,5.21,5.48) which shows that the entropy method gives acceptable foreign object distinguishing results.

3D imaging simulation

The SAR processing is also used to simulate the 3D images of the targets using a planar array of static antennas.

- Fig. 4 presents the baseline configuration used in this work. It consists of a rectangular antenna array located at $R = 20$m from the target. The transmitting array is made of a single transmitter located at the center of the antenna. The receiver array consists of 26 line receivers uniformly distributed along a 0.7m $\hat{z}$-aperture. Each line receiver is comprised of 46 single receivers uniformly distributed along a 1.85m $\hat{x}$-aperture.

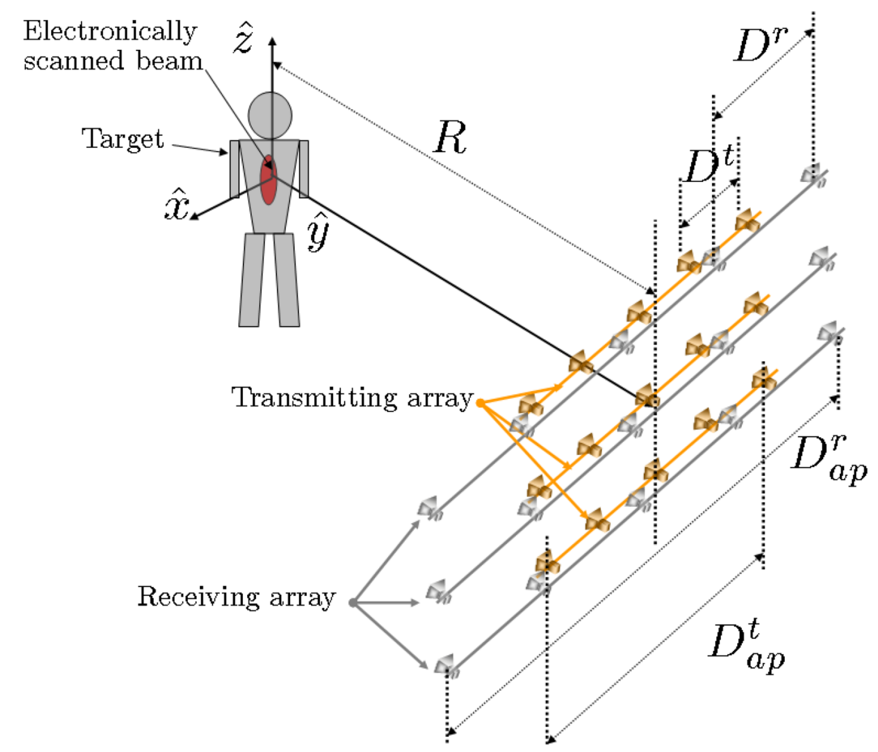

Figure 4: Antenna array and target configuration

- The study tested the image reconstruction algorithm against 2 different geometries: male body and male body with metallic cylindrical pipes on the chest (Fig. 6).
- The simulation treated the centroid of every triangular patch in the body mesh model as an individual point source. The intensity of each individual point source was proportional to the area of the corresponding triangular patch.
- In the case shown in Fig. 5(b), the 5 cylindrical metallic pipes have a radius $r = 0.01$m and a height $h = 0.2$ m.
- Figs. 6(a) and 6(b) show the reconstructed reflectivity of the observation space. Figs. 6(a) shows the reconstructed image for the body without metallic pipes. Figs. 6(b) shows the reconstructed images for the body with cylindrical metallic pipes on the chest. The difference between these two sceneraios is better displayed in Fig. 6(c) when we choose a higher threshold for the equiamplitude reflectivity.

Conclusion

In this poster we have presented our latest results in the area of standoff detection of potential suicide bombers. We have described the radar configuration for the standoff problem and the motion compensation algorithms used to improve the SAR image. We have used a feature detection algorithm, based on measuring the randomness of the image by means of its entropy, in order to distinguish between threat and no threat cases. The threat cases present a higher entropy value than no threat cases. We have also presented the imaging capabilities of a system composed of a two dimensional aperture of receiving antennas. The two dimensional array is able to generate 3D images, which substantially improves the probability of threat detection since an additional dimension is added to the SAR image.

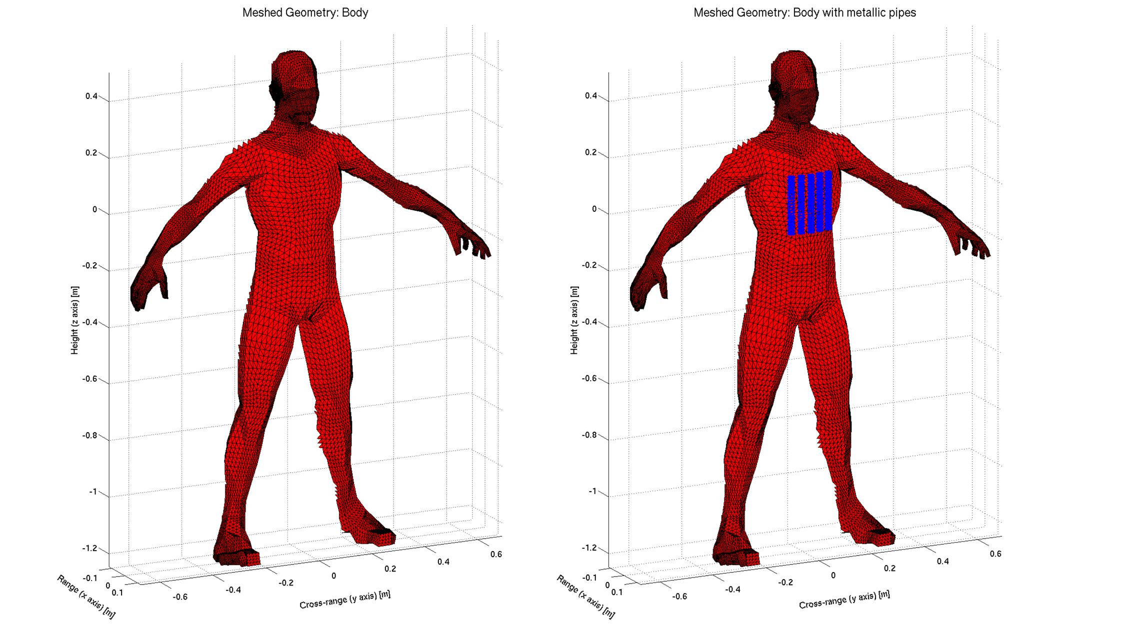

(a) (b)

Figure 5: Target geometry used in the simulation: (a) body without metallic pipes, and (b) body with metallic pipes

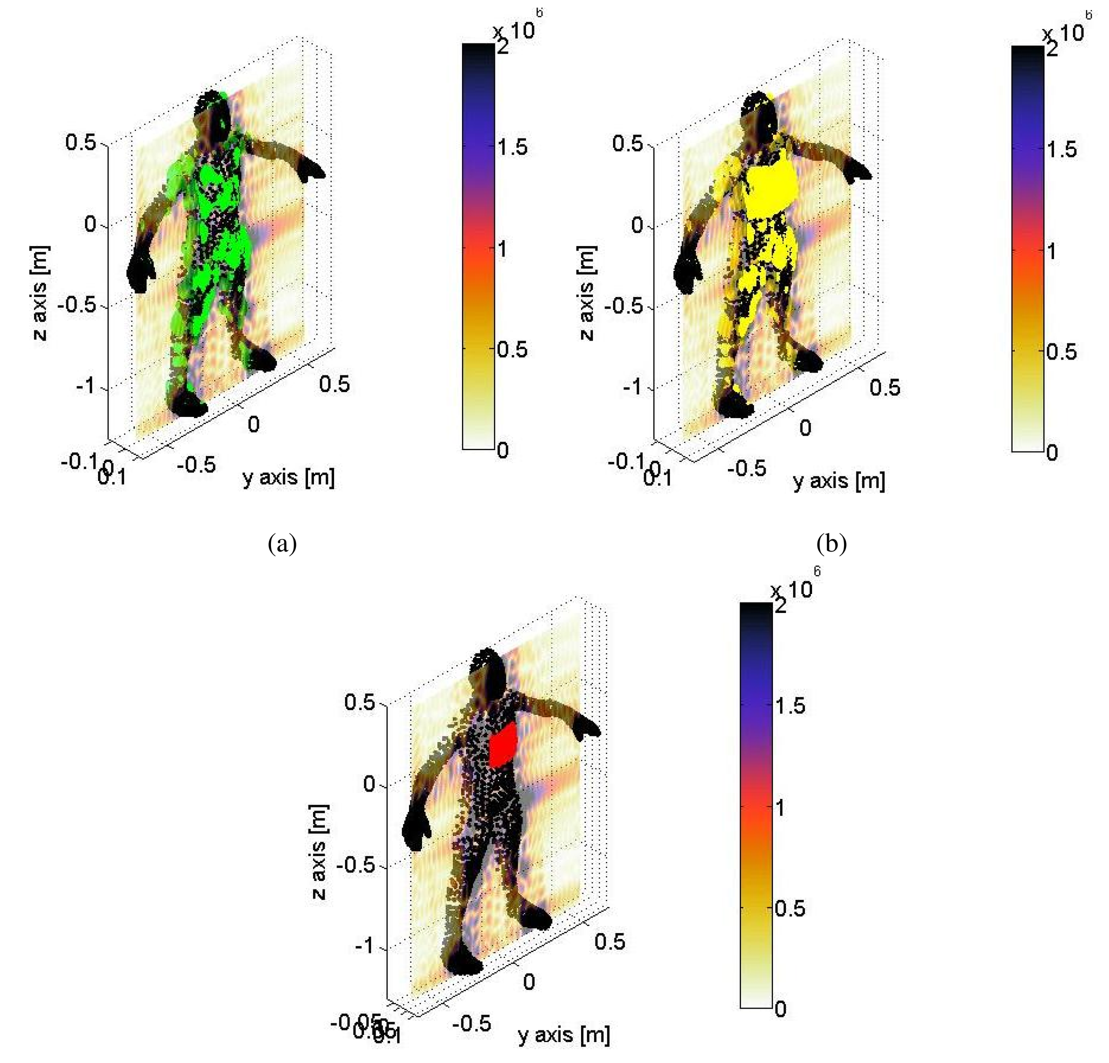

Figure 6: Image reconstruction: (a) Reflectivity and isocontours of body without metallic pipes (b) reflectivity and isocontours of body with 5 cylindrical metallic pipes (c)reflectivity and isocontours of body with 5 cylindrical metallic pipes with higher threshold

References

[1] Curlander J. C., McDonough R. N., Synthetic Aperture Radar: Systems and Signal Processing, John Wiley Sons, Inc., USA, 1991.

[2] Carrara W. G., Goodman R. S., Majewski R. M., Spotlight Synthetic Aperture Radar: Signal Processing Algorithms, Artech House, Inc., USA, 1995.

[3] Chen V. C., Ling H., Time-Frequency Transforms for Radar Imaging and System Analysis, Artech House Inc., USA, 2002.

Acknowledgments

This project was funded through the ALERT Center of Excellence under the Award Numbers (2008-ST-061-ED0001) and (2009-ST-108-000009) from the Department of Homeland Security, Science and Technology Directorate, Office of University Programs and International Cooperative Programs Office, respectively. The views and conclusions contained in this document are those of the authors and should not be interpreted as necessarily representing the official policies, either expressed or implied of the U.S. Department of Homeland Security.